Theoretical and Experimental Study of Inclusion Complexes Formed by Isoniazid and Modified β-Cyclodextrins: 1 H NMR Structural Determination and Antibacterial Activity Evaluation

ARTICLE *in* THE JOURNAL OF PHYSICAL CHEMISTRY B · DECEMBER 2013

Impact Factor: 3.3 · DOI: 10.1021/jp409579m · Source: PubMed

THE JOURNAL OF PHYSICAL CHEMISTRY B

Article

pubs.acs.org/JPCB

Theoretical and Experimental Study of Inclusion Complexes Formed by Isoniazid and Modified β-Cyclodextrins: ^{1}H NMR Structural Determination and Antibacterial Activity Evaluation

Milena G. Teixeira,[†] João V. de Assis,[‡] Cássia G. P. Soares,[†] Mateus F. Venâncio,[§] Juliana F. Lopes,[∥] Clebio S. Nascimento, Jr,[⊥] Cleber P. A. Anconi,[#] Guilherme S. L. Carvalho,[▽] Cristina S. Lourenço,[▽] Mauro V. de Almeida,[‡] Sergio A. Fernandes,[†] and Wagner B. de Almeida*[,§]

[†]Grupo de Química Supramolecular e Biomimética (GQSB), Departamento de Química, Universidade Federal de Viçosa (UFV), 36570-000, Viçosa, Minas Gerais, Brazil

[‡]Núcleo Multifuncional de Pesquisas Químicas (NUPEQ), Departamento de Química, Instituto de Ciências Exatas, Universidade Federal de Juiz de Fora (UFJF), 36036-330, Juiz de Fora, Minas Gerais, Brazil

[§]Laboratório de Computacional e Modelagem Molecular (LQC-MM), Departamento de Química, Universidade Federal de Minas Gerais (UFMG), 31270-901, Belo Horizonte, Minas Gerais, Brazil

[∥]Laboratório de Química Computacional (LaQC), Instituto de Física e Química, Universidade Federal de Itajubá (UNIFEI), 37500-903, Itajubá, Minas Gerais, Brazil

[⊥]Departamento de Ciências Naturais (DCNAT), Universidade Federal de São João Del Rei (UFSJ), Campus Dom Bosco, Praça Dom Helvécio, 74, 36301-160, São João Del Rei, Minas Gerais, Brazil

[#]Laboratório de Química Fundamental (LQF), Departamento de Química, Universidade Federal de Lavras (UFLA), Campus Universitário, 37200-000, Lavras, Minas Gerais, Brazil

[▽]Laboratório de Bacteriologia e Bioensaios em Micobactérias, Instituto de Pesquisa Clínica Evandro Chagas (IPEC) FIOCRUZ, 38659-508, Manguinhos, Rio de Janeiro, Brazil

ABSTRACT: Me-β-cyclodextrin (Me-βCD) and HP-β-cyclodextrin (HP-βCD) inclusion complexes with isoniazid (INH) were prepared with the aim of modulating the physicochemical and biopharmaceutical properties of the guest molecule, a well-known antibuberculosis drug. The architectures of the complexes were initially proposed according to NMR data Job plot and ROESY followed by density functional theory (DFT) calculations of ^{1}H NMR spectra using the PBE1PBE functional and 6-31G(d,p) basis set, including the water solvent effect with the polarizable continuum model (PCM), for various inclusion modes, providing support for the experimental proposal. An analysis of the ^{1}H NMR chemical shift values for the isoniazid (H6′,8′ and H5′,9′) and cyclodextrins (H3,5) C^{1}H hydrogens, which are known to be very adequately described by the DFT methodology, revealed them to be extremely useful, promptly confirming the inclusion complex formation. An included mode which describes Me-βCD partially enclosing the hydrazide group of the INH is predicted as the most favorable supramolecular structure that can be used to explain the physicochemical properties of the encapsulated drug. Antibacterial activity was also evaluated, and the results indicated the inclusion complexes are a potential strategy for tuberculosis treatment.

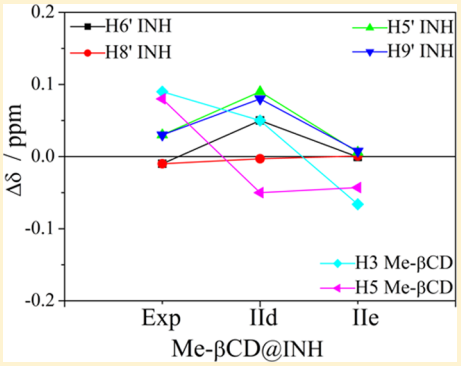

1. INTRODUCTION

Tuberculosis (TB) is a serious infectious disease and still a major concern for international health organizations.[1−4] The global number reached 9 million new cases in 2010 according to the World Health Organization,[4] and the number of new TB-infected people is increasing.[1] The TB treatment with isonicotinic hydrazide (INH, isoniazid, shown in Figure 1a)[5] was initiated in 1951 and presented a high specificity against TB bacteria. Novel approved chemotherapy treatment to tuberculosis is not observed because it is a neglected disease.[2−5] Pharmaceutical alternatives to isoniazid chemotherapy itself are needed, and in this sense, several ideas have been pursued. One of them is a drug combination such as the INH and rifampicin case, which was recently approved for TB treatment.[1] However, this strategy does not prevent the multidrug resistance mechanism that could appear in some patients. One alternative could be taking advantage of the host−guest chemistry to modulate the INH activity, improving features such as bioavailability and keeping its biological effect. Supramolecular systems[6−13] such as liposomes, crown ethers, cryptates,

Received: September 25, 2013
Revised: November 8, 2013
Published: December 9, 2013

   dx.doi.org/10.1021/jp409579m | J. Phys. Chem. B 2014, 118, 81−93

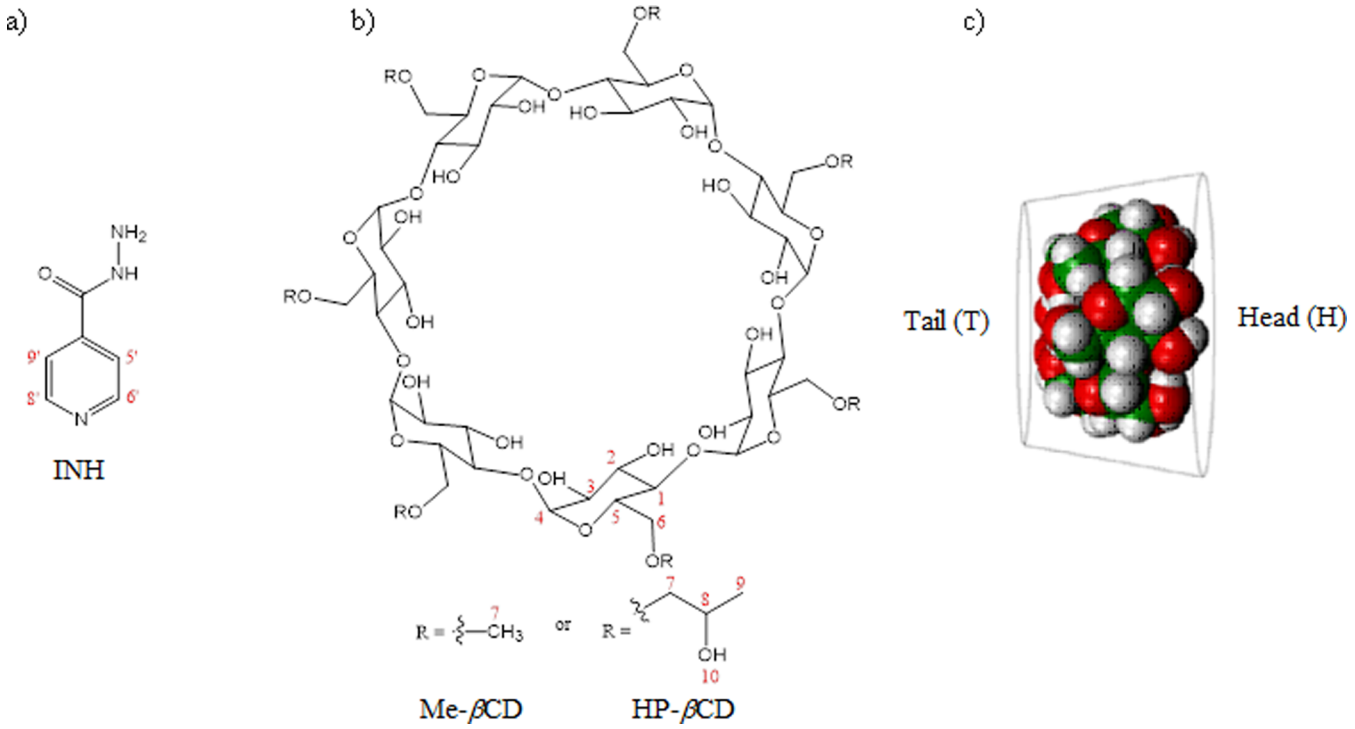

Figure 1. (a) Isoniazid structure, (b) structure of β-cyclodextrin and their derivatives, and (c) truncated cone topography of CDs with two different rims, a wider (head, H) and a narrower (tail, T). The assigned hydrogen atoms in this paper are also highlighted.

calix[n]arenes, and cyclodextrins have been used as drug-enclosing agents. In a previous work,[14] Fernandes and co-workers investigated the capacity of the sodium p-sulfonatocalix[4]arene and sodium p-sulfonatocalix[6]arene to form complexes with the isoniazid, and through the use of different ^{1}H NMR methodologies and theoretical calculations elucidated the structure and stabilization of such complexes. Another possibility, the INH inclusion by β-cyclodextrins derivatives, which has not been comprehensively and sufficiently investigated,[15] motivate this new study.

Cyclodextrins (CDs) are cyclic oligosaccharides formed by glucose units interconnected by α-(1,4) linkages (Figure 1b).[16] CD molecules can be pictured as a shallow truncated cone (Figure 1c).

This kind of structure provides a hydrophobic cavity of different sizes, depending on the number of elementary glucose units, and two different rims, a wider one (head, H) containing all secondary hydroxyl groups and a narrower one (tail, T) containing all primary hydroxyl groups. The difference between the primary and secondary hydroxyl groups allows selective functionalization on the primary and secondary rims. Selective modification of CDs has been extensively studied by many researchers[17,18] and has provided, among others, functionalized CDs, methyl-β-cyclodextrin (Me-βCD) and hydroxypropyl-β-cyclodextrin (HP-βCD) (Figure 1b). These two CDs have been highlighted because of their application as host in molecular inclusion processes with various nonpolar guest molecules.

The study of drug inclusion with pharmaceutical activity is one of the most extensively developing areas of research.[19,20] The main advantages in using CDs in pharmaceutical formulations include enhanced aqueous solubility, bioavailability, and stability.[21] The multiequilibrium of supramolecular systems is responsible for multiple complex arrangements in solution which are stabilized by intermolecular interactions.[22−25] Hence, the characterization without single-crystal analysis, which undoubtedly could provide data about the compound structure, often depends on the chemical interpretation of spectroscopic results such as NMR experiments. Because of these features, theoretical studies[9,24,26] can be very helpful because a molecular point of view can be accessed; therefore, a better understanding of the inclusion complexes structures is provided.

In this paper, a quantum chemical method is used jointly with NMR experiments to describe more precisely those inclusion complex structures obtained for INH and Me-βCD and HP-βCD. The experimental work of sample preparations and characterization followed by successful biological tests of antituberculosis activity of the presumed inclusion complex formed between isoniazid and functionalized cyclodextrins provides a motivation for carrying out the corresponding theoretical study using the density functional theory (DFT) method.[27] Comparisons between theoretical and experimental ^{1}H NMR chemical shifts, for free and complexed INH hydrogen atoms and also for Me-βCD inner hydrogen atoms, provided an interpretation of experimental NMR spectra on a solid basis, leading to an unambiguous proof of the formation of the inclusion complex.

2. MATERIALS AND METHODS

2.1. Chemicals and Reagents. Isoniazid (INH) (99%), hydroxypropyl-β-cyclodextrin (HP-βCD) (98%), methyl-β-cyclodextrin (Me-βCD) (98%), and D_2O (99.75%) were purchased from Sigma-Aldrich. All other reagents were of analytical grade.

2.2. Preparation of Solid Inclusion Complexes. Inclusion complexes (HP-βCD@INH and Me-βCD@INH) at 1:1 M ratio were obtained by mixing a 10 mmol L^{-1} aqueous solution of compounds HP-βCD or Me-βCD with a solution of

dx.doi.org/10.1021/jp409579m | J. Phys. Chem. B 2014, 118, 81−93

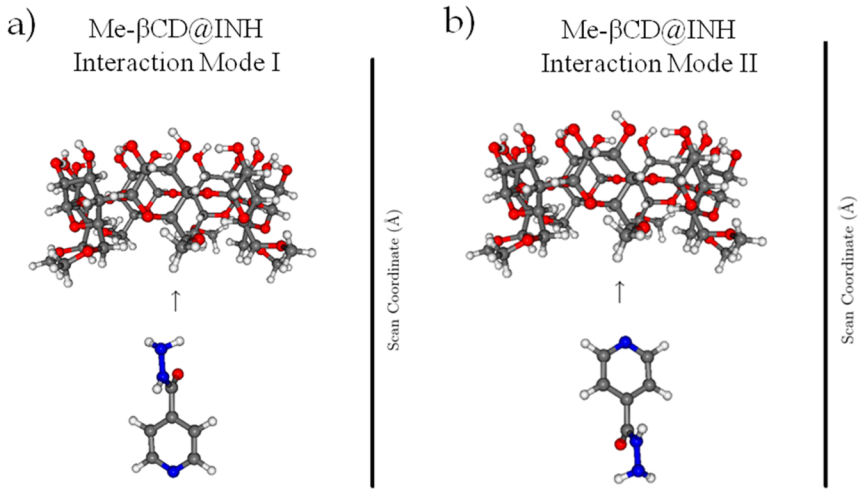

Figure 2. Me-βCD@INH inclusion complexes formation through the scan coordinate. (a) Interaction mode I, the hydrazide moiety approach and (b) interaction mode II, pyridine ring toward CD cavity.

10 mmol L^{-1} isoniazid (INH). Each system was stirred for 48 h at room temperature, a period of time considered as the optimum to reach equilibrium. Each solution was freeze-dried in a Labconco Freeze-dry System (Freezone 4.5) and stored at 253 K until further use.

2.3. NMR Spectroscopy. All experiments were performed at 298 K in D_2O.

2.3.1. Routine 1D. ^1H NMR spectra were acquired with a MERCURY-300 Varian spectrometer operating at 300.069 MHz for ^1H (64 k data points, 30° excitation pulse with duration of 2.2 μs, spectral width of 6 kHz, acquisition time of 3.3 s, and relaxation delay of 10 ms) in a 5 mm probe with direct detection mode at room temperature unless stated otherwise.

2.3.2. Determination of the Stoichiometry of Complexation. Job plots have been prepared with 10 mmol L^{-1} stock solutions of compounds INH, HP-βCD and Me-βCD.[28,29]

2.3.3. NOE Measurements. The ROESY 1D experiment was obtained with a selective 180° and a nonselective 90° pulse; a mixing time of 0.5 s was used during the spin-lock. The selective pulses were generated by a waveform generator, which automatically attenuates the shape, power, and pulse duration to obtain the required selectivity. The subtraction of the on- and off-resonance acquisition furnished the ROESY 1D experiment. All spectra were acquired with a 5 mm inverse probe at 298 K in 5 mm tubes.

2.4. Differential Scanning Calorimetry (DSC). The samples (10 mg) were placed in aluminum pans, and the experiments were run in a calorimeter (Universal V2.3D TA Instruments) at a 10 °C/min heating rate over a wide temperature range (0−250 °C). An empty pan served as reference, and indium was used to calibrate the temperature.

2.5. Theoretical Calculations. Initially the geometries of isolated isoniazid (orthogonal arrangement) and Me-βCD structures were fully optimized using a DFT methodolgy[26] employing the PBE1PBE functional[30,31] with the standard Poplés 6-31G(d,p) basis set[32,33] (PBE1PBE/6-31G(d,p)). Then a PBE1PBE/6-31G(d,p) energy scan, with both host and guest kept frozen at the optimized structure, for the interaction between INH and Me-βCD was carried out to locate the plausible minimum energy structures on the potential energy surface (PES). The scan coordinate (d) was chosen as a distance from the INH aromatic ring center and a dummy point situated in the middle of the CD, following a straight line perpendicular to the CD as described in Figure 2. The relative energy (E_{rel}) was evaluated as the total energy of the complex at a specific distance d subtracted from the energy of the complex having the INH placed at d = 15 Å from the middle of the CD cavity. This is the isolated structure configuration. In this way, E_{rel} is close enough to the complex formation energy from the free INH and Me-βCD molecules placed at a distance approaching infinity (ΔE). The stationary points found in this scan search were fully optimized without any constraint. Next, PBE1PBE/6-31G(d,p) calculations of nuclear magnetic resonance (NMR) spectra were carried out for all 10 different optimized structures of the Me-βCD@INH complexes located on the two calculated energy curves. The gauge-independent atomic orbital method (GIAO) implemented by Wolinski, Hinton, and Pulay[34] was used for the evaluation of NMR chemical shifts (δ) for selected hydrogen atoms obtained on the δ-scale relative to the TMS. In this work, HDO was used, replacing TMS. The solvent effect (water: ε = 78.39) was accounted for using the polarizable continuum model (PCM) by the integral equation formalism (IEFPCM)[35] in single-point calculations on the fully optimized geometries in the vacuum. All calculations were performed with the Gaussian-09 quantum mechanical package.[36]

2.6. Antitubercular Activity. The antimycobacterial activities of HP-βCD@INH and Me-βCD@INH complexes were assessed against *Mycobacterium tuberculosis* ATTC 27294[37] using the microplate Alamar blue assay (MABA).[38] This nontoxic methodology uses thermally stable reagents and shows good correlation with proportional and BACTEC radiometric methods.[39,40] Briefly, 200 mL of sterile deionized water was added to all outer-perimeter wells of sterile 96-well plates (Falcon, 3072: Becton Dickinson, Lincoln Park, NJ) to minimize evaporation of the medium in the test wells during incubation. The 96 plates received 100 μL of the Middlebrook 7H9 broth (Difco Laboratories, Detroit, MI) and a serial dilution of the compounds was made directly on the plate. The final drug concentrations tested were 0.01−10.0 μL mL^{-1}. Plates were covered and sealed with parafilm and incubated at 37 °C for five days. After this time, 25 μL of a freshly prepared 1:1 mixture of Alamar blue (AccuMed International, Westlake, OH) reagent and 10% Tween 80 were added to the plate and incubated for 24 hours. A blue color in the well was interpreted

dx.doi.org/10.1021/jp409579m | J. Phys. Chem. B 2014, 118, 81−93

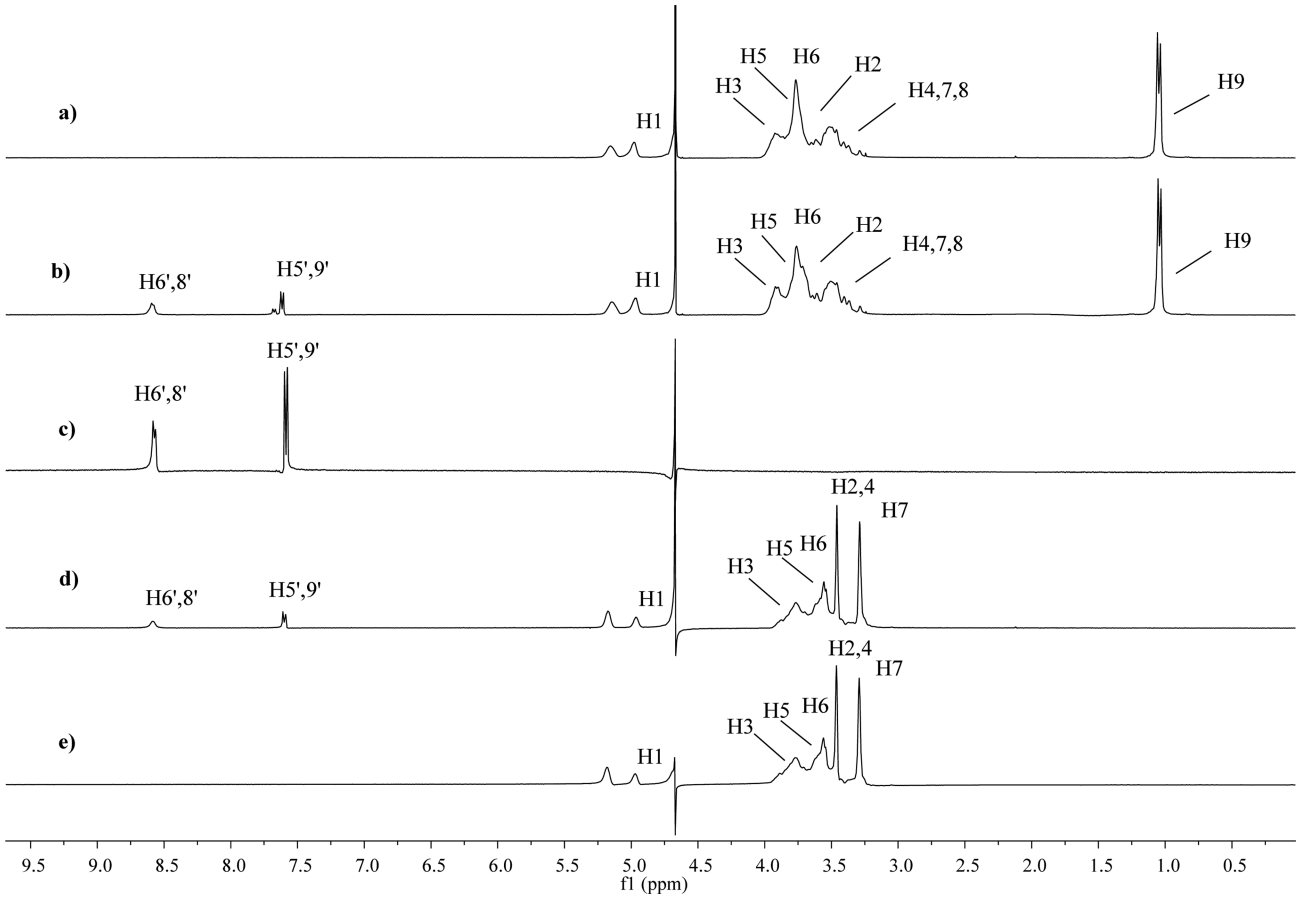

Figure 3. ^{1}H NMR spectra (300.069 MHz; D_2O; δ_{HDO} 4.67; 298 K; 10 mmol L^{-1} each): (a) HP-βCD, (b) HP-βCD@INH, (c) INH, (d) Me-βCD@INH, and (e) Me-βCD.

as absence of bacterial growth, and a pink color was scored as growth. The minimal inhibitory concentration (MIC) was defined as the lowest drug concentration to give 90% inhibition of bacterial growth, which prevented a color change from blue to pink.

3. RESULTS AND DISCUSSION

3.1. NMR Analysis. NMR techniques were employed to obtain detailed information about the interactions between the guest INH and the host HP-βCD or Me-βCD in aqueous solution. The ^{1}H NMR spectra for INH in D_2O in the presence or absence HP-βCD or Me-βCD were obtained (Figure 3).

Isoniazid hydrogen atoms (Figure 1a) were observed as a single resonance because of fast exchange between free and complexed guest molecules on the NMR time scale. The numbers corresponding to the NMR signals of all studied isolated species are shown in Table 1. We started our investigation by analyzing the complexation-induced hydrogen chemical shifts ($\Delta\delta$) in the HP-βCD@INH and Me-βCD@INH complexes in comparison to those of free isoniazid molecule.

Complexation between INH and HP-βCD and Me-βCD revealed that the guest molecule hydrogens show small variation of chemical shifts (Figure 3 and Table 1), indicating weak interaction between the guest and both hosts. We have also observed a relatively larger variation in the chemical shifts of both cyclodextrin hydrogens being more pronounced for H3 and H5 of the Me-βCD, as can be verified in Table 1. The molecular interactions taking place between guest and hosts

Table 1. ^{1}H NMR Data: Chemical Shifts (δ) and Chemical Shift Differences ($\Delta\delta = \delta_{INH\text{-}free} - \delta_{INH\text{-}complex}$)[a]

	INH	HP-βCD	HP-βCD@INH		Me-βCD	Me-βCD@INH	
hydrogens	δ	δ	δ	$\Delta\delta$	δ	δ	$\Delta\delta$
H5′,9′	7.59	–	7.62	−0.03	–	7.60	−0.01
H6′,8′	8.57	–	8.58	−0.01	–	8.54	0.03
H3	–	3.92	3.91	0.01	3.85	3.76	0.09
H5	–	3.77	3.76	0.01	3.80	3.72	0.08

[a]10 mmol L^{-1} samples, 298 K.

were further investigated by monitoring the chemical shifts of the H5′,9′ hydrogens of INH. Job plots were conducted for determining the stoichiometry of the complexation reactions. The plot for Me-βCD@INH, which is presented in Figure 4, showed a maximum at 0.5 guest/host molar ratio and is representative for the analogous inclusion complex formation with HP-βCD, indicating that 1:1 complexes (HP-βCD@INH and Me-βCD@INH) are formed[28,29] in aqueous solution.

1D ROESY NMR experiments were carried out to obtain complementary information on the inclusion geometries of the HP-βCD@INH and Me-βCD@INH complexes. Unlike complexation-induced shifts, ROESY cross-peaks are indicative of specific proximity relationships between guest and host hydrogens (generally 4 Å or less).[41] To gain more insight into the topological aspects of these two complexes, HP-βCD@INH and Me-βCD@INH, we have performed ^{1}H-ROESY NMR experiments, which are usually suited to measure NOEs in

dx.doi.org/10.1021/jp409579m | J. Phys. Chem. B 2014, 118, 81−93

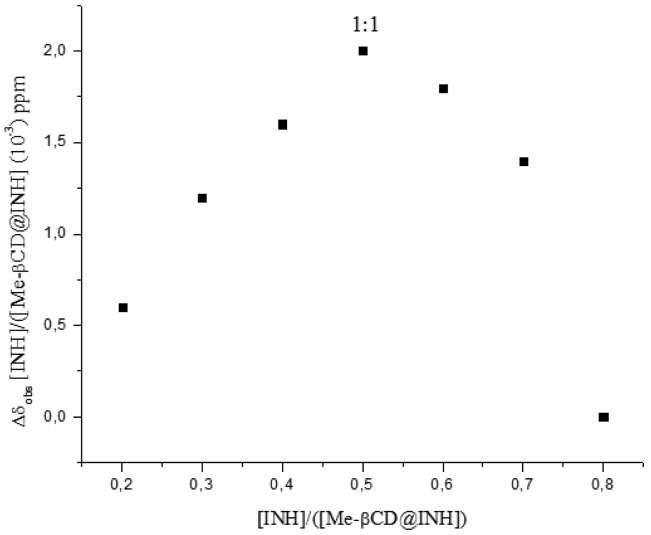

Figure 4. Representative Job plot for the inclusion complex formation for Me-βCD@INH.

complexes with $\omega\tau_c$ close to 1.[42] Specific ROE signals were observed between H5′,9′ of INH with H3 and H5 of HP-βCD and Me-βCD, respectively (Figure 5). Specific ROE signals were not observed between H6′,H8′ of INH and the host (HP-βCD and Me-βCD) (data not shown). We therefore propose that the INH hydrazide moiety is enclosed by the cyclodextrins cavity (Figure 5).

3.2. Differential Scanning Calorimetry (DSC). DSC thermograms were obtained to analyse the rate of heat absorbed by isoniazid, HP-βCD, Me-βCD, HP-βCD@INH and Me-βCD@INH physical mixtures, and HP-βCD@INH and Me-βCD@INH inclusion complexes (1:1 molar ratio). This analysis gave supporting evidence for the complexation of isoniazid with HP-βCD and Me-βCD. Figure 6 shows thermograms for isoniazid (Figure 6a), HP-βCD (Figure 6b), HP-βCD@INH physical mixture (Figure 6c), HP-βCD@INH solid complex (Figure 6d), Me-βCD (Figure 6e), Me-βCD@INH physical mixture (Figure 6f), and Me-βCD@INH solid complex (Figure 6g). For HP-βCD and Me-βCD, a peak corresponding to water loss was also observed (50 °C). A typical DSC curve for a crystalline anhydrous substance, with a sharp fusion endotherm (T peak = 168 °C), was obtained for isoniazid (Figure 6a). A similar peak can be observed by analyzing physical mixture thermal behavior (Figure 6c,f). The disappearance as well as the shift of endo- or exothermic peaks of drugs is a clear indication of the complexation phenomenon,[43] explaining the absence of the fusion peak of pure isonazid (168 °C) in the thermogram in Figure 6d,g. This result is evidence of the inclusion of the isoniazid molecule into the CD hydrophobic cavity.

3.3. Theoretical Calculations. Two distinct energy curves were obtained for two modes of approximation of the INH to the Me-βCD: through the hydrazide moiety (Figure 2a, mode I) and through the nitrogen atom belonging to the pyridine ring (Figure 2b, mode II). The potential energy curves presented in Figure 7 were a reliable tool for identifying 10 local minimum energy structures having $E_{rel} < 0$. The corresponding equilibrium distances are quoted in the caption of Figure 7.

These Me-βCD@INH equilibrium structure complexes were named "a" to "e" and fully optimized at the PBE1PBE/6-31G(d,p) level with the final optimized equilibrium structures shown in Figure 8. Not coincidently, these structures are representative of several possibilities of inclusion result because noncovalent bonds are formed; multiple equilibrium is expected.[22,24]

The PBE1PBE/6-31G(d,p) interaction energies (ΔE in kilocalories per mole) for the Me-βCD@INH complexes were calculated with eq 1 and are given in Table 2. In this equation, $E_{complex}$ is the total energy of the inclusion complex and the values in parentheses are the corresponding energies for the isolated INH and Me-βCD species at their fully optimized geometries. For the isoniazid molecule, the orthogonal structure (see Figure 2) was used as reference, which is the experimentally observed isomer as reported in ref 14. It is worth mentioning that INH could self-associate because it has hydrogen bond donors and acceptors. These intermolecular interactions were assumed to be weaker than those that will be formed with the solvent D_2O. The Job plot (Figure 4) also supports the fact that INH self-aggregation can be ignored, if present in solution, because the majority of complexes are 1:1. Also quoted in Table 2 are instantaneous interaction energy values (ΔE_{INS} in kilocalories per mole) estimated using eq 2, where for the INH and Me-βCD species, the energies are calculated from their separated structures at the optimized complex geometries and not from the isolated structures as described by the interaction energy ΔE. The ΔE_{INS} value can provide a description of the intermolecular interaction strength present in the stabilized inclusion complex that is more realistic than that of the energy of complex formation, ΔE. It can be seen from Table 2 that the inclusion complexes are not very strongly bound; the association complexes (**Ia**, **Ie**, **IIa**, and **IIe**) are quite weakly bound, and the fully included complexes, **Ic** and **IIc** structures, are relatively more stable. The ΔE_{INS} values show the same tendency; however, the association complexes are still very weakly bound. and probably they would not be stable enough to efficiently carry the drug through the biological media.

$$\Delta E = E_{complex} - (E_{INH} + E_{Me\text{-}\beta CD}) \quad (1)$$

$$\Delta E_{INS} = E_{complex} - (E_{INH} + E_{Me\text{-}\beta CD})_{complex\ geometries} \quad (2)$$

The solvent effect was modeled by the PCM model with the water dielectric constant simulating the solvent electrostatic effects on the solute. PCM solvent energies are also given in Table 2, and it can also be seen that, in the light of the PCM description of the solvent effect, the solvation energy contribution (ΔE^{Solv}), which is a measure of the complex stabilization due to solvent effects, is repulsive, making the formation of the complex not favorable on an energetic basis only. The same behavior is found for the ΔE_{INS} values, with a repulsive solvation energy term (ΔE^{Solv}_{INS}) of the same magnitude obtained. The interaction energy in the presence of the solvent ($\Delta E^{H_2O} = \Delta E + \Delta E^{Solv}$) is a positive number for all 10 complex structures. If a different solvent model was used, maybe the complex formation would not be destabilized by the solvent effect. Our results indicated that the PCM model may not be adequate to totally describe the solute−solvent interactions present in the inclusion process. The intermolecular interactions that take place inside the cyclodextrin cavity are specially ignored by the continuum model because the solvent-accessible area is modeled as a nonpenetrable region. However, intermolecular interactions that the whole complex is doing with the solution can be indirectly contemplated by this kind of

dx.doi.org/10.1021/jp409579m | J. Phys. Chem. B 2014, 118, 81−93

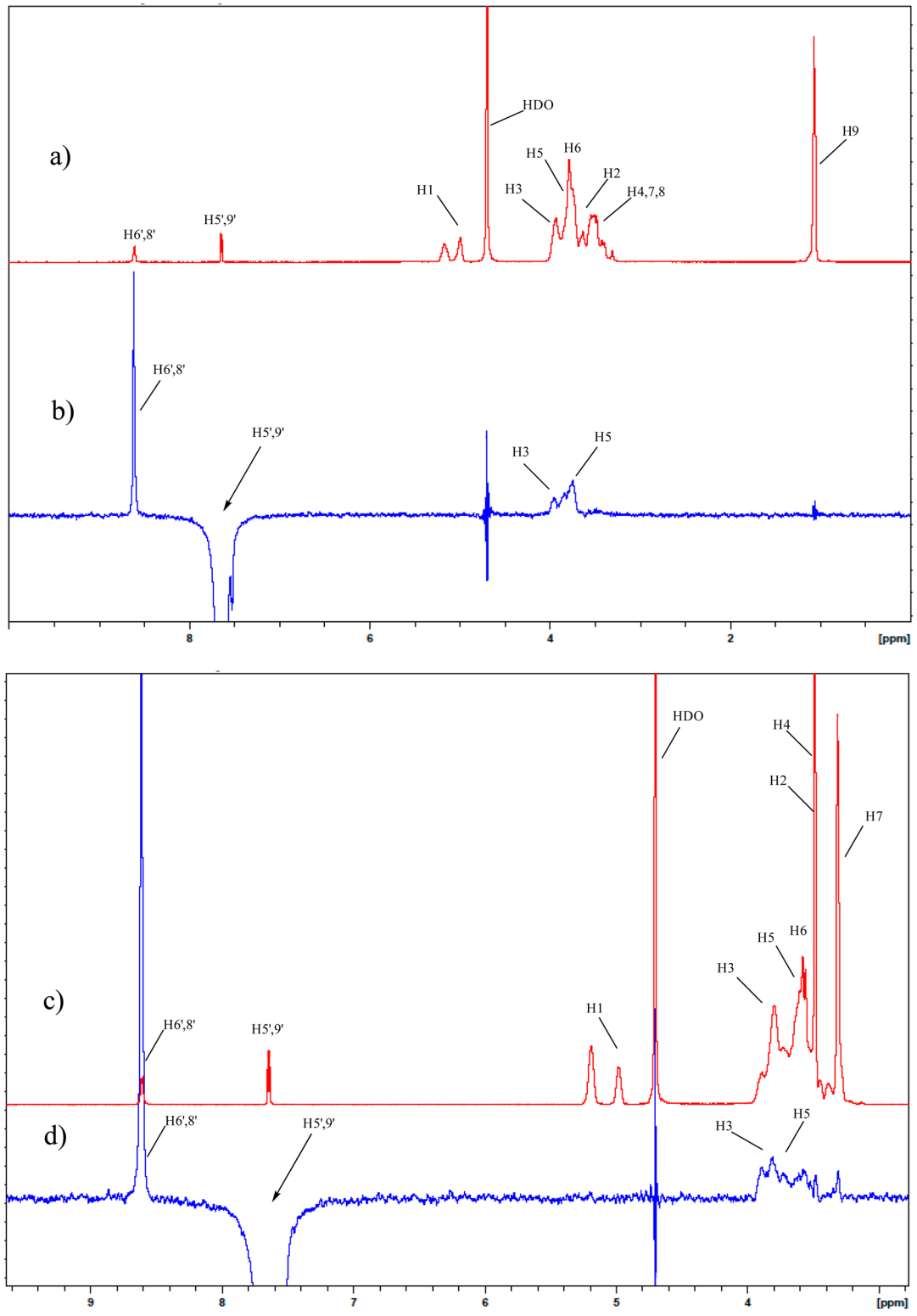

Figure 5. ^{1}H NMR spectra (400 MHz, D_2O, 298 K, 10 mmol L^{-1} each): (a) HP-βCD@INH, (b) representative 1D-ROESY spectra of irradiated H5′,9′ of INH, (c) Me-βCD@INH, and (d) representative 1D-ROESY spectra of irradiated H5′,9′ of INH.

solvent model. Additionally, the results shown in Table 2 indicate that the use of explicit solvent models through quantum mechanical calculations may be more adequate. On the other hand, for such large and conformationally flexible molecular systems this strategy can be computationally unviable. This warning is particularly important when a major concern of the work is to understand the thermodynamic contribution on the inclusion process. As our experience attested,[22−24,26] the presence of the explicit solvent water, or even the use of a method more elegant than implicit solvation, is not required for structural analysis of the inclusion complexes.

In a very recent work concerning the formation of an inclusion complex between cisplatin and a model carbon

dx.doi.org/10.1021/jp409579m | J. Phys. Chem. B 2014, 118, 81−93

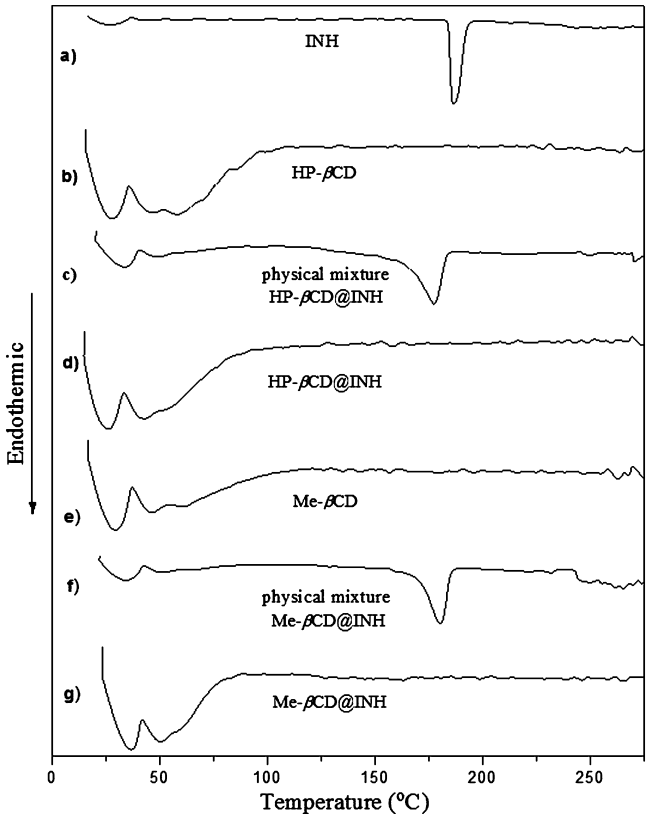

Figure 6. DSC thermograms: (a) isoniazid pure, (b) HP-βCD, (c) HP-βCD@INH physical mixture, (d) HP-βCD@INH solid complex, (e) Me-βCD, (f) Me-βCD@INH physical mixture, and (g) Me-βCD@INH solid complex.

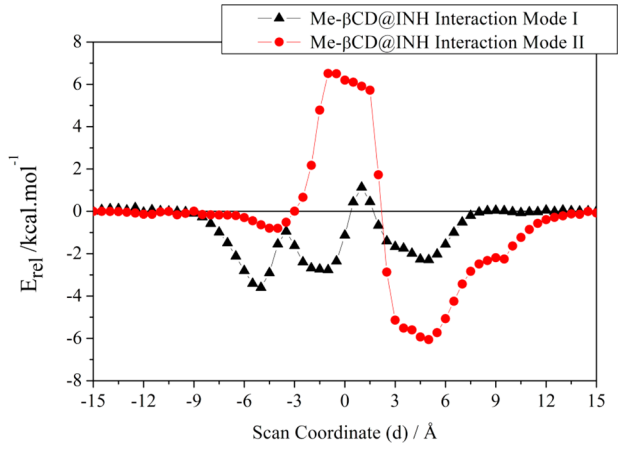

Figure 7. PBE1PBE/6-31G(d,p) potential energy curves for interaction modes I and II of Me-βCD@INH. Equilibrium distances: **Ia** (d = −12 Å), **Ib** (d = −5 Å), **Ic** (d = −1 Å), **Id** (d = 5 Å), **Ie** (d = 10.5 Å), **IIa** (d = −10 Å), **IIb** (d = −4 Å), **IIc** (d = 5 Å), **IId** (d = 9 Å), and **IIe** (d = 14 Å).

nanohorn,[44] a study of the interaction of cisplatin with a smaller model system, corannulene, allowed a comparison with accurate post-HF MP2[45,46]calculations to be made. It was shown that the M06-2x functional developed by Truhlar et al.[47] was in excellent agreement with MP2 results, with the B3LYP functional producing too small energy of formation values. Therefore, in the present work we also carried out M06-2x/6-31G(d,p) single-point calculations and geometry optimization for two structures, **IId** and **IIe**, that are representative of Me-βCD@INH complexes, as will be shown later. The results are given in Table 2 in brackets. It can be seen that the M06-2x functional increases remarkably the complex stabilization as compared with the PBE1PBE/6-31G(d,p) results, using the same optimized geometry (M06-2x single-point calculation). When the complex **IId** geometry is optimized at the M06-2x/6-31G(d,p) level, a huge increase in stabilization is observed (ΔE = −10.7 kcal mol^{-1}). A similar result was observed for the cisplatin−nanohorn and cisplatin−corannulene complex,[44] where electron correlation effects play an important role with the nature of the intermolecular interaction probably having a considerable contribution of dispersion forces. The M06-2x energy result reported in Table 2 strongly indicates that the Me-βCD@INH **IId** complex would have enough stabilization to be carried out through the biological media without premature dissociation into free monomers. It also shows how the complex formation energy (ΔE), calculated for a specific reaction model (see eq 1), can drastically vary by changing the DFT functional. The solvent effects (ΔE^{Solv}) calculated with the M06-2x and PBE1PBE functional are essentially the same; the same trend is observed for the instantaneous interaction energy (ΔE_{INS}).

It is worth mentioning that we have recently investigated the electrostatic and dispersion nature of the cisplatin−water complex and found that among various DFT functionals, the M06-2x demonstrated the best performance for describing electron correlation and dispersion effects as compared to the state-of-the-art coupled cluster with single, double, and perturbative triple excitations (CCSD(T))[48] higher correlated level results. The basis set superposition error (BSSE) effect[49] was also previously investigated, using the counterpoise method,[50] for cisplatin−water[51,52] and cisplatin−corannulene complexes[44] at the DFT and post-HF MP2 levels, showing that the MP2 BSSE correction is substantially larger than that of DFT, which becomes negligible as the basis set improves. It was concluded that M06-2x/6-31G(d,p) energies can be considered a reasonable estimate of the complex formation energy at an affordable computational cost. Therefore, M06-2x energies and BSSE correction values with three basis sets of increasing size, 6-31G(d,p),[32,33] 6-31++G(d,p), and 6-311++G(2d,2p)[32,33] (the later is of triple-ζ quality), calculated for the optimized **IId** and **IIe** geometries, are also reported in Table 2. A decrease in the BSSE value, 50%, 33%, and 24%, respectively, is observed for structure **IId**, as expected (see footnotes of Table 2). The BSSE corrected energies of complex **IId** formation (ΔE^{BSSEc}), using the 6-31G(d,p), 6-31++G(d,p), and 6-311++G(2d,2p) basis sets, are −5.4, −6.0, and −5.0 kcal mol^{-1}, respectively. So, an adequate value for the Me-βCD@INH **IId** complex should be around −6 kcal mol^{-1}, providing a good stabilization for the inclusion compound as required for experimental proposals.

The structural study is the initial step for the NMR calculations because the characterization of the inclusion modes obtained in solution is our main goal. In this sense, recent PCM chemical shift theoretical results reported for quebrachitol[53,54] and also calix[n]arenes inclusion complexes[14] provide support to the approach used in this work, consisting of DFT single-point NMR calculations using the PCM model with molecular geometries optimized in the vacuum. Changes in NMR chemical shift values for guest and host molecules due to complex formation can be used as strong evidence of the formation of inclusion complexes, as is exemplified in the case

dx.doi.org/10.1021/jp409579m | J. Phys. Chem. B 2014, 118, 81−93

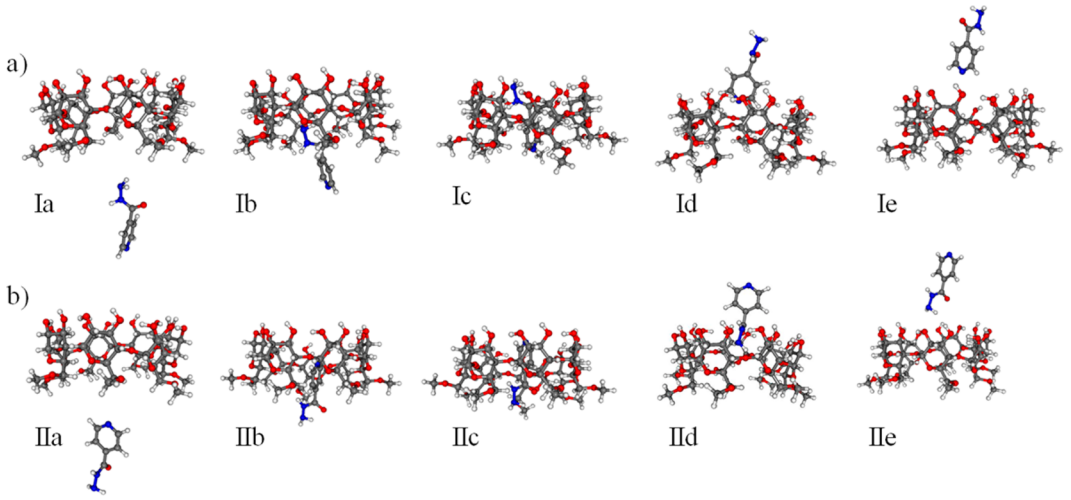

Figure 8. PBE1PBE/6-31G(d,p) fully optimized structures for (a) interaction mode I and (b) interaction mode II.

Table 2. PBE1PBE/6-31G(d,p) Energy of Formation for the Interaction between INH and Me-βCD, in Vacuum (ΔE) and Water (ΔE^{H_2O}), and the Solvent Effect Contribution (ΔE^{Solv}), for Two Interaction Modes[a]

complex	Ia	Ib	Ic	Id	Ie	IIa	IIb	IIc	IId	IIe
ΔE	0.01	−2.2	−3.5	−0.7	0.2	0.3	−2.2	−5.2	−0.6	−0.1
									[−1.6][e]	[0.1][e]
									[−10.7][f]	[−0.1][f]
									[−8.9][g]	[−0.7][g]
									[−7.8][h]	[−0.6][h]
ΔE^{H_2O}[b]	4.8	10.4	9.2	11.8	4.0	8.2	9.2	8.6	12.0	7.5
									[11.0][e]	[7.8][e]
									[0.9][f]	[8.2][f]
ΔE^{Solv}[c]	4.8	10.8	12.7	12.5	3.8	7.9	11.4	13.8	12.6	7.6
									[12.6][e]	[7.7][e]
									[11.6][f]	[8.3][f]
ΔE_{INS}[d]	−0.3	−1.6	−6.2	−2.6	−0.5	−0.1	−3.7	−6.7	−2.9	−0.2
									[−4.6][e]	[−0.2][e]
									[−13.4][f]	[−0.2][f]
$\Delta E_{INS}^{H_2O}$[b,d]	4.4	8.9	6.9	9.8	3.2	7.9	7.7	7.0	9.6	7.6
									[8.0][e]	[7.6][e]
									[−3.6][f]	[7.5][f]
ΔE_{INS}^{Solv}[c,d]	4.7	10.5	13.1	12.4	3.7	8.0	11.4	13.7	12.5	7.8
									[12.6][e]	[7.8][e]
									[9.8][f]	[7.7][f]

[a]M06-2x/6-31G(d,p) single-point values are quoted in brackets. All energy values in kilocalories per mole. The fully optimized structures are shown in Figure 8. [b]ΔE^{H_2O}: single-point PCM PBE1PBE/6-31G(d,p) energy difference using the fully optimized geometry in the vacuum. [c]The PCM solvation energy contribution: $\Delta E^{Solv} = \Delta E^{H_2O} - \Delta E$. [d]See eq 2, where frozen complex monomer geometries (not free monomer optimized) are used. [e]M06-2x/6-31G(d,p)//PBE1PBE/6-31G(d,p) single-point energy value. [f]M06-2x/6-31G(d,p) fully optimized geometry value. Structure **IId**: BSSE = 5.3 kcal mol^{-1} (50%). [g]M06-2x/6-31++G(d,p)//M06-2x/6-31G(d,p) single-point value. Structure **IId**: BSSE = 2.9 kcal mol^{-1} (33%). [h]M06-2x/6-311++G(2d,2p)//M06-2x/6-31G(d,p) single-point value. Structure **IId**: BSSE = 1.9 kcal mol^{-1} (24%).

of the study of molecular wires formed from polythiophenes and cyclodextrins.[55]

Theoretical and experimental ^{1}H NMR spectra for free isoniazid and Me-βCD are shown in Figure 9, with the specification of the hydrogen atom labels for the analysis of ^{1}H NMR spectra given in Figure 1. Presuming a full inclusion of the guest molecule, only the inner hydrogen atoms (H3 and H5) of cyclodextrin are relevant for the analysis of chemical shift variations due to complex formation. The H3 and H5 experimental ^{1}H NMR signals for the free Me-βCD monomer are virtually the same, while the theoretical (DFT) values show a sizable splitting of approximately 0.2 ppm, what may be explained probably due to a dynamic change of position of these hydrogen atoms leading to the observation of an average value. The theoretical quantum chemical calculation is based on a static structure, and so the H3 and H5 hydrogen atoms are exposed to fixed distinct chemical environment. Therefore, a good agreement between theory and experiment can be assumed for the free Me-βCD. For the free isoniazid, the agreement for the H6′,8′ hydrogen atoms is perfect with a shift of ∼0.5 ppm observed for H5′,9′ with respect to the experimental value. From Figures 1 and 2 it can be seen that the H5′,9′ hydrogen atoms are near the hydrazide group, causing a deviation of the PBE1PBE/6-31G(d,p) theoretical value calculated using the PCM model to simulate the solvent effects (water) in relation to the signal observed in the

dx.doi.org/10.1021/jp409579m | J. Phys. Chem. B 2014, 118, 81−93

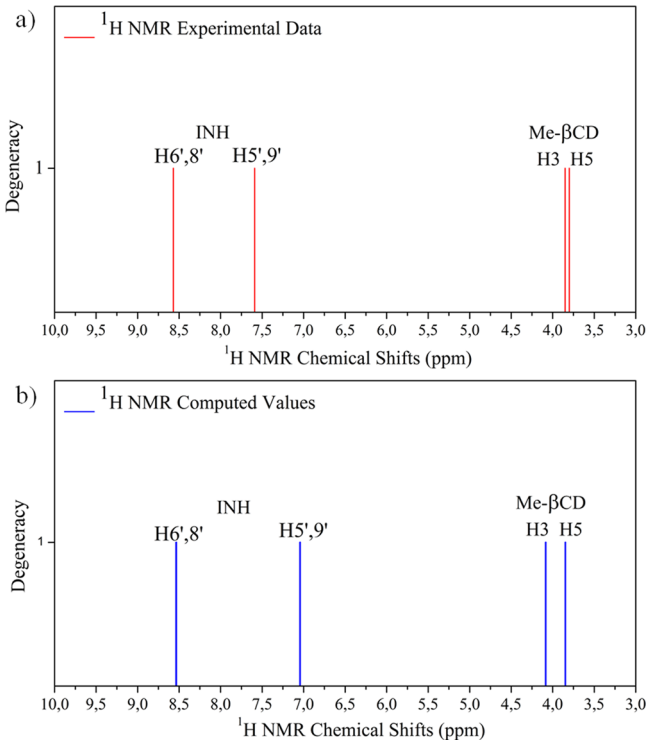

Figure 9. Free isoniazid and Me-βCD ^{1}H NMR spectra. The H3, H5 (Me-βCD), and H5′,9′, H6′,8′ hydrogen atoms from INH are shown in Figure 1. (a) Experimental data (in D_2O) and (b) theoretical results (PBE1PBE/6-31G(d,p) PCM values).

experimental sample (D_2O). As stated before, a strategy to improve the theoretical results could be a refinement of the geometry optimization procedure with a tight convergence criterion and also the use of other noncontinuum solvation model, including explicit water molecules, to describe the solvent effects for the DFT calculation of the GIAO nuclear magnetic shielding tensors. However, such a procedure would not be computationally viable for a large molecular system such as the Me-βCD@INH inclusion complexes. Despite this relatively small deviation, which is naturally expected when spectroscopic data evaluated using a theoretical model are compared to experimental values, the agreement between theory and experiment for the free INH and Me-βCD can be considered very good; therefore, the DFT NMR chemical shifts are shown to be adequate for the further analysis of the inclusion complexes.

The experimental ^{1}H NMR spectrum, measured in D_2O, for the Me-βCD@INH complex and the PBE1PBE/6-31G(d,p) PCM theoretical values calculated for the 10 different optimized complex structures located on the PES are shown in Figure 10. The definition of hydrogen labels are given in Figure 1 The spatial view of each optimized structure is shown in Figure 8. The deviation between the experimental ^{1}H NMR spectrum for complex and free monomers is small (an observed shift of 0.01−0.09 ppm), so they are qualitatively the same.

It can be seen from Figure 10 that the effect of changes in the molecular complex structure have a noticeable effect on ^{1}H NMR chemical shifts that can be promptly identified by experimental measures. Therefore, the complex structure showing the least deviation from the experimental data should be the preferred structure experimentally observed. A similar procedure was used successfully by our group in a recent work on calix[n]arene complexes.[14] It can be seen that all four association modes (**Ia**, **Ie**, **IIa**, **IIe**), which are very weakly bound, show a very reasonably agreement with experiment, as does the partially included complex structure **IId**, which resembles **IIe**, where the hydrazide moiety is interacting with the Me-βCD cavity as indicated by the analysis of the experimental ROESY NMR data. So these molecular structures are natural candidates to outline the probable multiple equilibrium present in the experimental sample handled in the NMR experiment. It is important to mention that the calculated M06-2x/6-31G(d,p) molecular structure and ^{1}H NMR spectra for structures **IId** and **IIe** are essentially the same as the PBE1PBE/6-31G(d,p) results. Only the interaction energy, which is more sensitive to the level of calculation than molecular geometry and NMR chemical shifts, is substantially altered by changing the DFT functional.

A more quantitative analysis of the theoretical ^{1}H NMR chemical shifts can be accomplished with the results of chemical shift differences ($\Delta\delta = \delta_{1\ \mathrm{free}} - \delta_{1\ \mathrm{complex}}$) for the inclusion complexes (experimental values in 10 mmol L^{-1} samples, 298 K) reported in Tables 3 and 4. It can be seen from Table 3 that the $\Delta\delta$ values for all four adsorption complexes are small and in very reasonable quantitative agreement with experimental values, keeping in mind that a variation in theoretical chemical shift values of ∼0.01−0.09 ppm is probably within the uncertainty of the theoretical methodology. In spite of this , the very large theoretical $\Delta\delta$ figures for some hydrogens, being more than 5 or 10 times the respective experimental values exhibited by the **Ib**, **Id**, **IIb**, **Ic**, and **IIc** partial or full inclusion complexes is certainly a well-justified criterion for ruling them out. The partially included complex structure **IId** is the only nonassociation mode of complexation that exhibits a good agreement with experimental $\Delta\delta$ values, with a perceptible disagreement being caused by the opposite sign of some chemical shift differences leading to a larger calculated deviation between theory and experiment. The observed $\Delta\delta$ values are very small; therefore, because a correct sign of such a small quantity is hard to attain using a theoretical methodology, a better way to analyze the variation of ^{1}H NMR chemical shifts due to complex formation is to use absolute difference deviations $\Delta(|\Delta\delta|)$ for Me-βCD@INH complexes with respect to the experimental values. These results are given in Table 4. The average $\Delta(|\Delta\delta|)$ values reported in the last row of Table 4 show an adequate statistical deviation between theoretical and experimental chemical shift values, and comparison of these chemical shift differences for the 10 inclusion complex structures shown in Figure 2 clearly shows that the partially included **IId** complex is the best candidate to be the experimentally observed inclusion complex structure, as indicated from the analysis of the experimental NMR spectra. The small average deviation between experimental and theoretical chemical shift difference values of 0.05 ppm reported in Table 4 for Me-βCD@INH complex **IId** can be considered more than sufficient to validate the assignment of the experimentally observed inclusion complex structure based only on the analysis of experimental and theoretical ^{1}H NMR spectra. The M06-2x/6-31G(d,p) stabilization energy for structure **IId** reported in Table 2 corroborates the NMR results.

Figure 11 shows a compilation of $\Delta\delta$ values for all 10 inclusion complexes investigated here, where it can promptly be seen that all nonadsorption complexes, except structure **IId**, exhibit a very large deviation from the experimental chemical shift profile and therefore can be discarded. The numerical

dx.doi.org/10.1021/jp409579m | J. Phys. Chem. B 2014, 118, 81−93

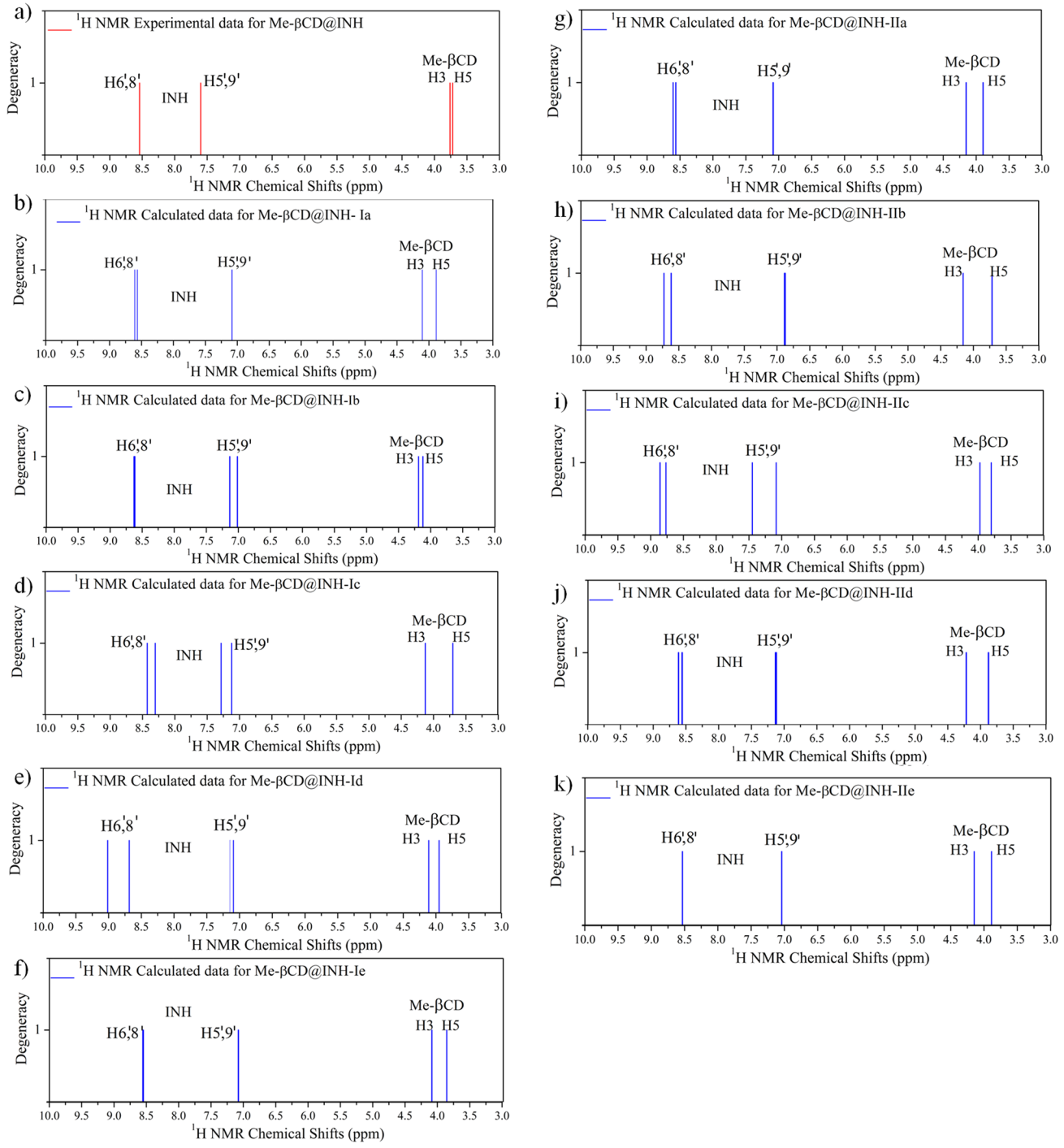

Figure 10. ^{1}H NMR spectra for Me-*β*CD@INH inclusion complex: (a) experimental data (in D_2O) and (b–k) theoretical results (PBE1PBE/6-31G(d,p) PCM) for distinct complex orientations.

results reported in Tables 3 and 4 may be better visualized in Figure 11, where a good agreement with experiment for all adsorption complexes (**Ia**, **Ie**, **IIa**, **IIe**), in spite of the sign of $\Delta\delta$, and also for the partially included complex structure **IId** is clearly seen. The spatial view of the PBE1PBE/6-31G(d,p) optimized structure of the **IId** complex, which matches the experimentally proposed topology of the inclusion complexes, through the hydrazide moiety and based on ^{1}H NMR chemical shift evidence (measured in D_2O), is shown in Figure 8b. The good match between theoretical predictions based on DFT calculations and experimentally deduced complex structure from the analysis of ^{1}H NMR data is a very welcome result and stresses the importance of complementary theoretical and experimental works.

3.4. Antitubercular Activity. Table 5 shows the minimal inhibitory concentration (MIC) of the inclusion complexes against *M. tuberculosis*. The results showed that the complexes exhibit biological activity similar to first-line drugs such as isoniazid (INH) and rifampicin (RIP) and clearly could be considered a good starting point for further studies as well as for finding new lead compounds. Therefore, the spectroscopic and complex stabilization analysis reported in this work,

dx.doi.org/10.1021/jp409579m | J. Phys. Chem. B 2014, 118, 81–93

Table 3. PBE1PBE/6-31G(d,p) ^{1}H NMR Chemical Shift Differences ($\Delta\delta = \delta_{1\ free} - \delta_{1\ complex}$) for Me-$\beta$CD@INH Inclusion Complexes (Experimental Values in 10 mmol L^{-1} samples, 298 K)

	experimental data, $\Delta\delta^{a,b}$	theoretical data, $\Delta\delta$									
		Ia[c]	Ib[d]	Ic[e]	Id[d]	Ie[c]	IIa[c]	IIb[d]	IIc[e]	IId[d]	IIe[c]
H6′	0.03	−0.03	−0.09	0.11	−0.15	−0.02	−0.03	−0.19	−0.23	0.05	−0.001
H8′	0.03	−0.07	−0.11	0.23	−0.48	−0.02	−0.07	−0.09	−0.32	−0.003	0.001
H5′	−0.01	−0.03	−0.10	−0.23	−0.09	−0.03	−0.03	0.16	−0.40	0.09	0.006
H9′	−0.01	−0.03	0.02	−0.07	−0.04	−0.04	−0.03	0.17	−0.03	0.08	0.007
H3-βCD	0.09	−0.02	−0.05	−0.04	−0.02	−0.02	−0.06	−0.07	0.12	0.05	−0.07
H5-βCD	0.08	−0.04	−0.35	0.15	−0.10	−0.02	−0.04	0.13	0.05	−0.05	−0.04

[a]Experimental value. [b]$\Delta\delta = \delta_{free} - \delta_{complex}$ [c]Adsorption mode of complexation. [d]Partial inclusion mode of complexation. [e]Full inclusion mode of complexation.

Table 4. PBE1PBE/6-31G(d,p) ^{1}H NMR Chemical Shift Absolute Difference Deviations $\Delta(|\Delta\delta|)$ for Me-βCD@INH Inclusion Complexes, with Respect to the Experimental $\Delta\delta$ Values

	experimental data, $\Delta(|\Delta\delta|)^{a,b}$	theoretical data, $\Delta(|\Delta\delta|)^b$									
		Ia[c]	Ib[d]	Ic[e]	Id[d]	Ie[c]	IIa[c]	IIb[d]	IIc[e]	IId[d]	IIe[c]
H6′	0	0	0.06	0.08	0.12	−0.01	0	0.16	0.2	0.05	−0.029
H8′	0	0.04	0.08	0.2	0.45	−0.01	0.04	0.06	0.29	−0.003	−0.029
H5′	0	0.02	0.09	0.22	0.08	0.02	0.02	0.15	0.39	0.07	−0.004
H9′	0	0.02	0.01	0.06	0.03	0.03	0.02	0.16	0.02	0.06	−0.003
H3-βCD	0	−0.07	−0.04	−0.05	−0.07	−0.07	−0.03	−0.02	0.03	0.05	−0.02
H5-βCD	0	−0.04	0.27	0.07	0.02	−0.06	−0.04	0.05	−0.03	−0.05	−0.04
average[f]		0.04	0.12	0.13	0.20	0.04	0.03	0.12	0.22	0.05	0.02

[a]Experimental value. [b]$\Delta(|\Delta\delta|) = |\Delta\delta_{Theor}| - |\Delta\delta_{Expt}|$ [c]Adsorption mode of complexation. [d]Partial inclusion mode of complexation (Symmetrical Strucutre, New-Z-Matrix). [e]Full inclusion mode of complexation. [f]Average = $(\sum_i (\Delta(|\Delta\delta|)_i)^2/6)^{1/2}$

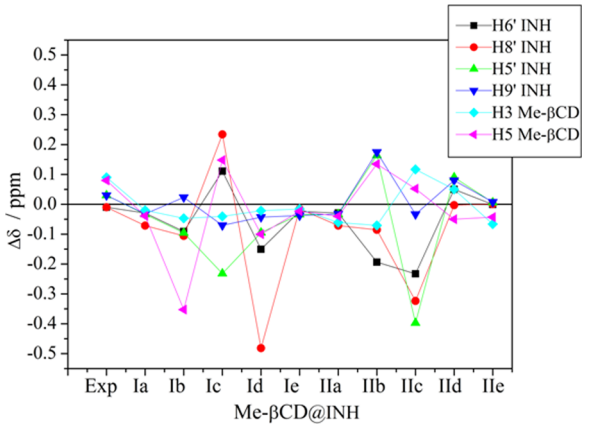

Figure 11. PBE1PBE/6-31G(d,p) ^{1}H NMR chemical shift differences ($\Delta\delta = \delta_{1\ free} - \delta_{1\ complex}$) for Me-$\beta$CD@INH inclusion complexes.

Table 5. MICs of INH and Inclusion Complexes against *M. tuberculosis* H37Rv Strain (ATCC 27294, Susceptible Both to Rifampicin and Isoniazid)

samples	MIC_{90} (μmol L^{-1})
INH	1.5
HP-βCD@INH	1.6
Me-βCD@INH	1.7
RIP	1.2

confirming the formation of an inclusion compound, will provide strong motivation for further experimental studies.

4. CONCLUSION

The present study addressed the preparation, physicochemical characterization and in vitro assays for the inclusion complexes HP-βCD@INH and Me-βCD@INH, followed by theoretical calculations using the DFT methodology. The NMR techniques employed in this work were crucial for the elucidation of the host−guest structure of both complexes. The complexation of INH with either HP-βCD or Me-βCD was investigated in view of their potential use for the preparation of new therapeutic formulations aiming to increase the drug bioavailability.

The proposed topologies of the complexes were initially established using experimental data from ROESY 1D. Major topics interest in the development of drug delivery system are the understanding of the specific features which determine the interaction between host−guest molecules and the study of the molecular aspects involved in such inclusion complexation phenomenon. Therefore, 10 plausible inclusion complex arrangements for Me-βCD@INH were optimized using the PBE1PBE/6-31G(d,p) level of calculation and the corresponding ^{1}H NMR chemical shift values calculated using the PCM model to simulate the water solvent effects. As a result, a good match between theoretical and experimental chemical shift profiles was found for a partially included complex structure (**IId**) which nicely fits to the experimental proposed topology, suggesting an intermolecular interaction through the hydrazide moiety based on ^{1}H NMR evidence. An association mode also reproduces very well the experimentally observed NMR profile. However, the strength of its intermolecular interaction is too weak to keep the inclusion complex bound in a biological environment, according to the theoretical DFT interaction energy calculations; therefore, equilibrium of both structures

dx.doi.org/10.1021/jp409579m | J. Phys. Chem. B 2014, 118, 81−93

can be representative of the experimental sample. In this sense the use of the M06-2x functional produced substantial stabilization of inclusion complex **IId**, and as reported previously by our group, it seems more adequate for the description of the energetics of inclusion compound formation. The Me-βCD@INH complex structure was elucidated through a combined experimental and theoretical DFT NMR investigation, and we can extrapolate this analysis to the HP-βCD@INH complexe arrangements based on the experimental data. This combined experimental and theoretical spectroscopic and energetic analysis confirming the formation of an inclusion compound will very likely stimulate further experimental studies which can effectively contribute to the development of new antituberculosis drugs.

AUTHOR INFORMATION

Corresponding Author

*Departamento de Química, Universidade Federal de Minas Gerais (UFMG), 31270-901, Belo Horizonte, MG, Brazil. Tel.: +55 31 34095776. Fax: +55 31 34095700. E-mail: wbdealmeida@gmail.com.

Notes

The authors declare no competing financial interest.

ACKNOWLEDGMENTS

The authors would like to thank to Dr. Anita Jocelyne Marsaioli for helping on NMR experiments. This work was supported by CNPq, FAPEMIG, FUNARBE, and CAPES. This work is part of a collaborative research project of members of the Rede Mineira de Química (RQ-MG) supported by FAPEMIG (Project REDE-113/10).

REFERENCES

(1) Shehzad, A.; Rehman, G.; Ul-Islam, M.; Khattak, W. A.; Lee, Y. S. Challenges in the development of drugs for the treatment of tuberculosis. *Braz. J. Infect. Dis.* **2013**, *17* (1), 74−81.

(2) Ekins, S.; Freundlich, J. S.; Choi, I.; Sarker, M.; Talcott, C. Computational databases, pathway and cheminformatics tools for tuberculosis drug discovery. *Trends Microbiol.* **2011**, *19* (2), 65−74.

(3) Balganesh, T. S.; Alzari, P. M.; Cole, S. T. Rising standards for tuberculosis drug development. *Trends Pharmacol. Sci.* **2008**, *29* (11), 576−581.

(4) http://www.who.int/research/en/. World Health Organization (accessed December 2011).

(5) Meyer, H.; Mally, J. Hydrazine derivatives of pyridine-carboxylic acids. *Monatsh. Chem.* **1912**, *33*, 393−414.

(6) Da Silva, D. L.; Tavares, E. D.; Conegero, L. D.; de Fatima, A.; Pilli, R. A.; Fernandes, S. A. NMR studies of inclusion complexation of the pyrrolizidine alkaloid retronecine and *p*-sulfonic acid calix[6]arene. *J. Inclusion Phenom. Macrocyclic Chem.* **2011**, *69* (1−2), 149−155.

(7) De Araújo, D. R.; Tsuneda, S. S.; Cereda, C. M. S.; Carualho, F. D. F.; Prete, P. S. C.; Fernandes, S. A.; Yokaichiya, F.; Franco, M.; Mazzaro, I.; Fraceto.; et al. Development and pharmacological evaluation of ropivacaine-2-hydroxypropyl-β-cyclodextrin inclusion complex. *Eur. J. Pharm. Sci.* **2008**, *33* (1), 60−71.

(8) Fernandes, S. A.; Cabeça, L. F.; Marsaioli, A. J.; de Paula, E. Investigation of tetracaine complexation with beta-cyclodextrins and *p*-sulphonic acid calix[6]arenes by nOe and PGSE NMR. *J. Inclusion Phenom. Macrocyclic Chem.* **2007**, *57* (1−4), 395−401.

(9) Rodrigues, S. G.; Chaves, I. D.; de Melo, N. F. S.; de Jesus, M. B.; Fraceto, L. F.; Fernandes, S. A.; de Paula, E.; de Freitas, M. P.; Pinto, L. D. A. Computational analysis and physico-chemical characterization of an inclusion compound between praziquantel and methyl-β-cyclodextrin for use as an alternative in the treatment of schistosomiasis. *J. Inclusion Phenom. Macrocyclic Chem.* **2011**, *70* (1−2), 19−28.

(10) Fraceto, L. F.; Gonçalves, M. M.; Moraes, C. M.; Araújo, D. R. d.; Zanella, L.; Paula, E. d.; Pertinhez, T. d. A. Caracterização do complexo de inclusão ropivacaína: β-ciclodextrina. *Quím. Nova* **2007**, *30*, 1203−1207.

(11) Arantes, L. M.; Scarelli, C.; Marsaioli, A. J.; de Paula, E.; Fernandes, S. A. Proparacaine complexation with β-cyclodextrin and *p*-sulfonic acid calix[6]arene, as evaluated by varied ^{1}H-NMR approaches. *Magn. Reson. Chem.* **2009**, *47* (9), 757−763.

(12) Fernandes, S. A.; Tavares, E. D.; Teixeira, R. R.; da Silva, C. M.; Montanari, R. M.; de Fatima, A.; Anconi, C. P. A.; de Almeida, W. B.; dos Santos, H. F.; da Silva, A. A. Inclusion complexes of Schiff bases as phytogrowth inhibitors. *J. Inclusion Phenom. Macrocyclic Chem.* **2013**, *75* (1−2), 197−204.

(13) Cabeca, L. F.; Fernandes, S. A.; de Paula, E.; Marsaioli, A. J. Topology of a ternary complex (proparacaine-β-cyclodextrin-liposome) by STD NMR. *Magn. Reson. Chem.* **2008**, *46* (9), 832−837.

(14) De Assis, J. V.; Teixeira, M. G.; Soares, C. G. P.; Lopes, J. F.; Carvalho, G. S. L.; Lourenco, M. C. S.; de Almeida, M. V.; de Almeida, W. B.; Fernandes, S. A. Experimental and theoretical NMR determination of isoniazid and sodium *p*-sulfonatocalix[*n*]arenes inclusion complexes. *Eur. J. Pharm. Sci.* **2012**, *47* (3), 539−548.

(15) Terekhova, I. V.; Kumeev, R. S. Thermodynamics of Inclusion Complexes between Cyclodextrins and Isoniazid. *Russ. J. Phys. Chem. A* **2010**, *84* (1), 1−6.

(16) Szejtli, J. Introduction and general overview of cyclodextrin chemistry. *Chem. Rev.* **1998**, *98* (5), 1743−1753.

(17) Engeldinger, E.; Armspach, D.; Matt, D. Capped cyclodextrins. *Chem. Rev.* **2003**, *103* (11), 4147−4173.

(18) Khan, A. R.; Forgo, P.; Stine, K. J.; D'Souza, V. T. Methods for selective modifications of cyclodextrins. *Chem. Rev.* **1998**, *98* (5), 1977−1996.

(19) Loftsson, T.; Brewster, M. E. Pharmaceutical applications of cyclodextrins 0.1. Drug solubilization and stabilization. *J. Pharm. Sci.* **1996**, *85* (10), 1017−1025.

(20) Loftsson, T.; Brewster, M. E. Cyclodextrins as functional excipients: Methods to enhance complexation efficiency. *J. Pharm. Sci.* **2012**, *101* (9), 3019−3032.

(21) Davis, M. E.; Brewster, M. E. Cyclodextrin-based pharmaceutics: Past, present and future. *Nat. Rev. Drug Discovery* **2004**, *3* (12), 1023−1035.

(22) De Paula, E. E. B.; De Sousa, F. B.; Da Silva, J. C. C.; Fernandes, F. R.; Melo, M. N.; Frezard, F.; Grazul, R. M.; Sinisterra, R. D.; Machado, F. C. Insights into the multi-equilibrium, superstructure system based on β-cyclodextrin and a highly water soluble guest. *Int. J. Pharm.* **2012**, *439* (1−2), 207−215.

(23) De Sousa, F. B.; Denadai, A. M. L.; Lula, I. S.; Lopes, J. F.; Dos Santos, H. F.; De Almeida, W. B.; Sinisterra, R. D. Supramolecular complex of fluoxetine with β-cyclodextrin: An experimental and theoretical study. *Int. J. Pharm.* **2008**, *353* (1−2), 160−169.

(24) Passos, J. J.; De Sousa, F. B.; Lula, I. S.; Barreto, E. A.; Lopes, J. F.; De Almeida, W. B.; Sinisterra, R. n. D. Multi-equilibrium system based on sertraline and β-cyclodextrin supramolecular complex in aqueous solution. *Int. J. Pharm.* **2012**, *421* (1), 24−33.

(25) Schatz, J. Recent application of ab initio calculations on calixarenes and calixarene complexes. A review. *Collect. Czech. Chem. Commun.* **2004**, *69* (6), 1169−1194.

(26) De Sousa, F. B.; Leite Denadai, A. M.; Lula, I. S.; Nascimento, C. S., Jr.; Fernandes Neto, N. S. G.; Lima, A. C.; De Almeida, W. B.; Sinisterra, R. D. Supramolecular self-assembly of cyclodextrin and higher water soluble guest: Thermodynamics and topological studies. *J. Am. Chem. Soc.* **2008**, *130* (26), 8426−8436.

(27) Parr, R. G.; Yang, W. *Density-Functional Theory of Atoms and Molecules*. Oxford University Press: Oxford, 1989.

(28) Fielding, L. Determination of association constants (K_a) from solution NMR data. *Tetrahedron* **2000**, *56* (34), 6151−6170.

(29) Job, P. *Annali di Chimica Applicata* **1928**, *9*, 113−203.

(30) Perdew, J. P. Density-Functional Approximation for the Correlation-Energy of the Inhomogeneous Electron-Gas. *Phys. Rev. B* **1986**, *33* (12), 8822−8824.
(31) Perdew, J. P.; Burke, K.; Ernzerhof, M. Generalized gradient approximation made simple. *Phys. Rev. Lett.* **1996**, *77* (18), 3865−3868.
(32) Hariharan, P. C.; Pople, J. A. Influence of Polarization Functions on Molecular-Orbital Hydrogenation Energies. *Theor. Chim. Acta* **1973**, *28* (3), 217−272.
(33) Hehre, W. J.; Ditchfield, R.; Pople, J. A. Self-Consistent Molecular Orbital Methods. XII. Further Extensions of Gaussian-Type Basis Sets for Use in Molecular Orbital Studies of Organic Molecules. *J. Chem. Phys.* **1972**, *56* (5), 2257−2261.
(34) Wolinski, K.; Hinton, J. F.; Pulay, P. Efficient Implementation of the Gauge-Independent Atomic Orbital Method for NMR Chemical-Shift Calculations. *J. Am. Chem. Soc.* **1990**, *112* (23), 8251−8260.
(35) Cances, E.; Mennucci, B.; Tomasi, J. A new integral equation formalism for the polarizable continuum model: Theoretical background and applications to isotropic and anisotropic dielectrics. *J. Chem. Phys.* **1997**, *107* (8), 3032−3041.
(36) Frisch, M. J.; Trucks, G. W.; Schlegel, H. B.;ScuseriaG. E.; Robb, M. A.; Cheeseman, J. R.; Scalmani, G.; Barone, V.; Mennucci, B.; Petersson, G. A.; Nakatsuji, H.; et al. *Gaussian 09*, revision A.02; Gaussian, Inc.: Wallingford CT, 2009.
(37) Canetti, J.; Rist, E.; Grosset, R. Measurement of sensitivity of the tuberculous bacillus to antibacillary drugs by the method of proportions. Methodology, resistance criteria, results and interpretation. *Revue de tuberculose et de pneumologie* **1963**, *27*, 217.
(38) Franzblau, S. G.; Witzig, R. S.; McLaughlin, J. C.; Torres, P.; Madico, G.; Hernandez, A.; Degnan, M. T.; Cook, M. B.; Quenzer, V. K.; Ferguson, R. M.; et al. Rapid, low-technology MIC determination with clinical Mycobacterium tuberculosis isolates by using the microplate Alamar Blue assay. *J. Clin. Microbiol.* **1998**, *36* (2), 362−366.
(39) Reis, R. S.; Neves, I.; Lourenco, S. L. S.; Fonseca, L. S.; Lourenco, M. C. S. Comparison of flow cytometric and alamar blue tests with the proportional method for testing susceptibility of *Mycobacterium tuberculosis* to rifampin and isoniazid. *J. Clin. Microbiol.* **2004**, *42* (5), 2247−2248.
(40) Vanitha, J. D.; Paramasivan, C. N. Evaluation of microplate Alamar blue assay for drug susceptibility testing of *Mycobacterium avium* complex isolates. *Diagn. Microbiol. Infect. Dis.* **2004**, *49* (3), 179−182.
(41) Pavia, D. L.; Lampman, G. M.; Kriz, G. S.; Vyvyan, J. R. *Introduction to Spectroscopy*. 4th ed.; Cole Cengage: Belmont, CA, 2009.
(42) Gunther, H. *NMR Spectroscopy*. 2nd ed.; John Wiley & Sons: Chichester, U.K., 1994.
(43) Loukas, Y. L.; Vraka, V.; Gregoriadis, G. Drugs, in cyclodextrins, in liposomes: A novel approach to the chemical stability of drugs sensitive to hydrolysis. *Int. J. Pharm.* **1998**, *162* (1−2), 137−142.
(44) De Souza, L. A.; Nogueira, C. A. S.; Lopes, J. F.; Dos Santos, H. l. F.; De Almeida, W. B. DFT study of cisplatin@carbon nanohorns complexes. *J. Inorg. Biochem.* **2013**, *129* (0), 71−83.
(45) Hehre, W. J.; Radom, L.; Schleyer, P. V. R.; Pople, J. A. *Ab initio Molecular Orbital Theory*. Wiley: New York, 1986.
(46) Szabo, A.; Ostlund, N. S. *Modern Quantum Chemistry, Introduction to Advanced Electronic Structure Theory*; Dover Publications Inc.: New York, 1996.
(47) Zhao, Y.; Truhlar, D. G. The M06 suite of density functionals for main group thermochemistry, thermochemical kinetics, noncovalent interactions, excited states, and transition elements: Two new functionals and systematic testing of four M06-class functionals and 12 other functionals. *Theor. Chem. Acc.* **2008**, *120* (1−3), 215−241.
(48) Bartlett, R. J.; Stanton, J. F. *Applications of Post-Hartree-Fock Methods: A Tutorial*. V. C. H. Publishers: New York, 1994; Vol. *5*, pp 65−169.
(49) van Duijneveldt, F. B.; van Duijneveldt-van de Rijdt, J. G. C. M.; van Lenthe, J. H. State-of-the-Art in Counterpoise Theory. *Chem. Rev.* **1994**, *94* (7), 1873−1885.
(50) Boys, S. F.; Bernardi, F. The Calculation of Small Molecular Interactions by Differences of Separate Total Energies. Some Procedures with Reduced Errors. *Mol. Phys.* **1970**, *19* (4), 553−&.
(51) Lopes, J. F.; Rocha, W. R.; Dos Santos, H. F.; De Almeida, W. B. Theoretical study of the potential energy surface for the interaction of cisplatin and their aquated species with water. *J. Chem. Phys.* **2008**, *128* (16), 14.
(52) Lopes, J. F.; Rocha, W. R.; dos Santos, H. F.; de Almeida, W. B. An Investigation of the BSSE Effect on the Evaluation of Ab Initio Interaction Energies for Cisplatin-Water Complexes. *J. Braz. Chem. Soc.* **2010**, *21* (5), 887−896.
(53) De Almeida, M. V.; Couri, M. R. C.; De Assis, J. V.; Anconi, C. P. A.; Dos Santos, H. F.; De Almeida, W. B. ^{1}H NMR analysis of O-methyl-inositol isomers: A joint experimental and theoretical study. *Magn. Reson. Chem.* **2012**, *50* (9), 608−614.
(54) De Almeida, M. V.; De Assis, J. V.; Couri, M. R. C.; Anconi, C. P. A.; Guerreiro, M. C.; Dos Santos, H. F.; De Almeida, W. B. Experimental and Theoretical Investigation of Epoxide Quebrachitol Derivatives Through Spectroscopic Analysis. *Org. Lett.* **2011**, *12* (23), 5458−5461.
(55) Venâncio, M. F.; Nascimento, C. S.; Anconi, C. P. A.; Lopes, J. F.; Rocha, W. R.; Dos Santos, H. F.; De Almeida, W. B. Theoretical Study of Spectroscopic Properties of Insulated Molecular Wires Formed by Substituted Oligothiophenes and Cross-Linked alpha-Cyclodextrin. *J. Polym. Sci., Part B: Polym. Phys.* **2011**, *49* (15), 1101−1111.